Room temperature charge and orbital ordering and phase coexistence in $Bi_{0.5}Sr_{0.5}MnO_3$

2001 J. Phys.: Condens. Matter 13 1071

(http://iopscience.iop.org/0953-8984/13/5/320)

INSTITUTE OF PHYSICS PUBLISHING JOURNAL OF PHYSICS: CONDENSED MATTER

J. Phys.: Condens. Matter **13** (2001) 1071–1078 www.iop.org/Journals/cm PII: S0953-8984(01)19607-4

Room temperature charge and orbital ordering and phase coexistence in $Bi_{0.5}Sr_{0.5}MnO_3$

C Frontera[1], J L García-Muñoz[1], A Llobet[1,2], M A G Aranda[3], C Ritter[4], M Respaud[5] and J Vanacken[6]

[1] Institut de Ciència de Materials de Barcelona, CSIC, Campus de la UAB, E-08193 Bellaterra, Spain
[2] Laboratoire Louis Néel, CNRS 25 Avenue des Martyrs, BP 166, 38042 Grenoble Cédex 9, France
[3] Departamento de Química Inorgánica, Cristalografía y Mineralogía Universidad de Málaga, PO Box 59 29071, Málaga, Spain
[4] Institut Laue–Langevin, 38042 Grenoble-Cédex, France
[5] SNCMP and LPMC, INSA, Complexe Scientifique du Rangueil, F-31077 Toulouse, France
[6] Laboratorium voor Vaste-Stoffysica en Magnetisme, Katholieke Universiteit Leuven, Celestijnenlaan 200 D, B-3001 Leuven, Belgium

E-mail: frontera@icmab.es

Received 28 November 2000

Abstract

We present high-resolution neutron and synchrotron powder diffraction, magnetotransport, and magnetization measurements on $Bi_{0.5}Sr_{0.5}MnO_3$. We report that, for the whole range of temperature 1.5 K $\leqslant T \leqslant$ 300 K, the sample studied exhibits coexistence of two phases. The majority phase presents charge and orbital order at least below 350 K. The existence and stability of charge order up to this high temperature agrees with the fact that magnetic fields higher than 45 T are not sufficient to melt the charge-ordered state at 4 K. This is in great contrast with the behaviour of non-Bi-based $Ln_{1/2}Sr_{1/2}MnO_3$ isostructural oxides.

1. Introduction

Mixed-valence manganites with perovskite structure have been attracting wide interest during the last decade. In manganites with general formula $Ln_{1-x}M_xMnO_3$ (Ln = trivalent lanthanide; M = divalent alkaline earth: Ca, Sr, Ba), the doping level x controls the proportion of Mn atoms in the Mn^{4+} oxidation state. In addition to the technologically powerful colossal-magnetoresistance effect, two very attractive phenomena exhibited by manganese perovskites are the charge order (CO) and the orbital order (OO). Ingredients such as Coulomb repulsion, the effect of Jahn–Teller distortion on the e_g energy levels, lattice distortions arising from electron–lattice interactions, and the strength of the double-exchange interaction play an important role in the stability of the CO state. When no OO is present, the dominant magnetic interaction is the ferromagnetic (FM) double exchange due to the strong Hund

coupling of the itinerant e_g electrons with the t_{2g} ones. When, following charge localization, OO takes place, then the dominant magnetic couplings are the superexchange interactions. These superexchange interactions are FM if a half-filled $d_{3r_i^2-r^2}$ ($r_i = x, y$, or z) and an empty e_g orbital are involved, and antiferromagnetic (AFM) if the orbitals involved are two t_{2g} orbitals [1–3]. The existence of AFM order in a perovskite manganite is normally associated with the existence of OO in it. It has been widely established that the CO transition is governed by the bandwidth of the e_g electrons [4, 5]. This bandwidth is controlled by the mean A-site cationic radius ($\langle R_A \rangle$): low $\langle R_A \rangle$ reduces the e_g bandwidth, favouring CO and OO.

The bismuth-based manganites $Bi_{1-x}M_xMnO_3$ behave quite differently to the rare-earth-based analogues. Although Bi^{3+} ($R_i^{IX} = 1.24$ Å) and La^{3+} ($R_i^{IX} = 1.22$ Å) have very similar ionic radii in many isostructural compounds [6], $LaMnO_3$ is AFM with A-type order and crystallizes in an orthorhombic cell (*Pbnm* or *Pnma* space group [7]). Conversely $BiMnO_3$ is ferromagnetic and crystallizes in a monoclinic cell (*C*2 space group [8]). Differences are also present in the Ca-doped samples: at low temperature $Bi_{2/3}Ca_{1/3}MnO_3$ is antiferromagnetic and insulating while $La_{2/3}Ca_{1/3}MnO_3$ is ferromagnetic and metallic [9]. These differences could be related to the particular electronic structure of the Bi^{3+} ions, having a highly polarizable $6s^2$ lone pair.

In this paper we study $Bi_{0.5}Sr_{0.5}MnO_3$ by means of synchrotron x-ray powder diffraction (SXRPD), neutron powder diffraction (NPD), and resistivity and magnetization measurements in the 1.5 K $\leqslant T \leqslant$ 300 K temperature interval. We have found that the system presents CO and OO over the whole temperature range. This result is quite surprising since the largest T_{CO} reported for a Sr-half-doped manganite is $T_{CO} \approx 165$ K [10], for the Nd-based perovskite.

2. Experimental details

Polycrystalline samples were sintered by standard solid-state reaction in air. Powders of $SrCO_3$, Bi_2O_3, and Mn_2O_3 were mixed at the desired ratios. The initial mixture was decarbonated at 900 °C for seven hours. After pressing the powder into pellets we carried out several firing processes at 1200 °C in air for 15 h each, separated by intermediate regrinding and pressing. The quality of the samples was initially checked by means of laboratory x-ray powder diffraction. Moreover, we collected NPD data using the D2B ($\lambda = 1.542$ Å) diffractometer at the Institut Laue–Langevin (Grenoble, France) at $T = 1.5$ and 300 K. SXRPD data were collected on the BM16 diffractometer at the ESRF (Grenoble, France) in the Debye–Scherrer (transmission) configuration at $T = 170$ and 300 K. Using a double-crystal Si(111) monochromator we selected the wavelength $\lambda = 0.442\,377(2)$ Å (calibrated with NIST Si). The patterns were refined by the Rietveld method using the programs GSAS [11] and FULLPROF [12]. We carried out a joint refinement of the neutron and synchrotron data collected at $T = 300$ K.

Resistivity measurements were made by the four-probe method using a commercial PPMS (Quantum Design) over the temperature range 4 K $\leqslant T \leqslant$ 350 K. DC magnetization data were obtained using an extraction magnetometer for the same temperature interval. In addition, high-magnetic-field magnetization measurements were performed at the facilities of the LVSM (Katholieke Universiteit of Leuven). Using the discharge of a bank capacitor in the coil, pulsed fields up to 50 T are obtained with a duration time of 20 ms.

3. Results and discussion

Figure 1(a) shows the temperature dependence of the electrical resistivity in zero magnetic field and under a field of $\mu_0 H = 8$ T. Two important features of the $\rho(T)$ curves displayed in

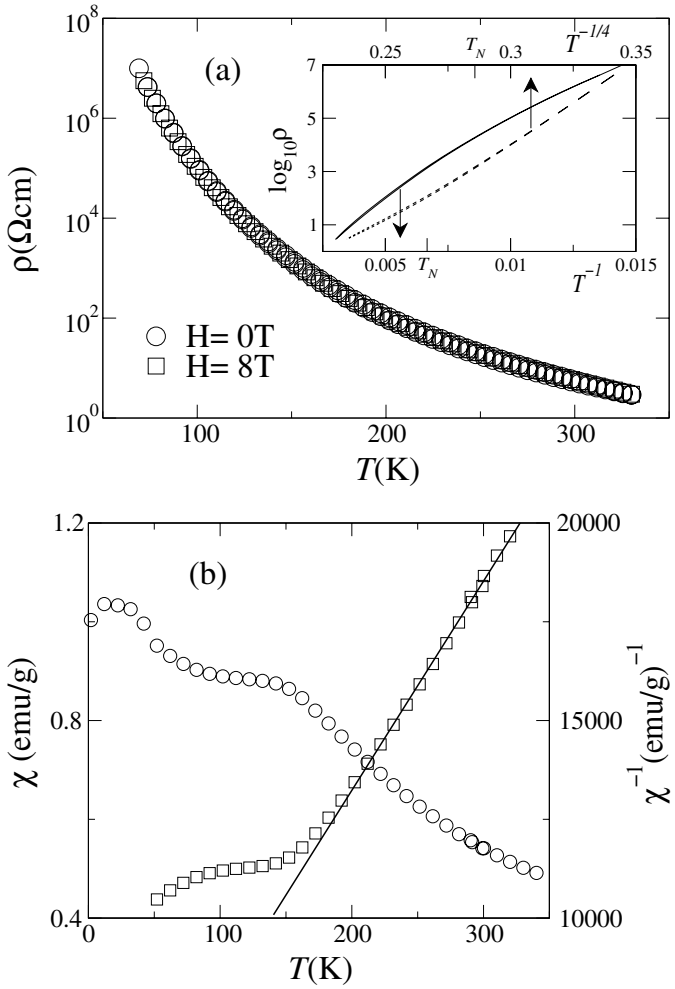

Figure 1. (a) Temperature dependence of the electrical resistivity at zero field (○) and with $H = 8$ T (□). The inset shows a plot of $\log_{10}\rho$ versus T^{-1} (solid line, bottom axis) and versus $T^{-1/4}$ (dashed line, top axis). T is in K and ρ in Ω cm. (b) Temperature dependence of the magnetic susceptibility (○) and its inverse (□). The straight line is the best fit of the Curie law.

figure 1(a) must be emphasized. These are as follows:

(i) $\rho(T)$ shows no transitions in the region displayed. It is of interest to note that the resistivity, even at RT, is considerable ($\rho(T) \sim 10^7$ Ω cm at $T = 80$ K). For comparison, the magnitude of the resistivity in polycrystalline $Pr_{0.5}Sr_{0.5}MnO_3$ remains moderately low in the semiconducting phase ($\sim 10^{-1}$ Ω cm and ~ 1 Ω cm at RT and 5 K respectively) [13, 14]. In fact, the high value of ρ prevented us from measuring it below $T \sim 80$ K. This large resistivity is typical of manganites with charge and orbital ordering ($\rho(T = 100\ \text{K}) \sim 10^3$–$10^4$ Ω cm for $Nd_{0.5}Ca_{0.5}MnO_3$, and 10^4 Ω cm for $Y_{0.5}Ca_{0.5}MnO_3$ and $Gd_{0.5}Ca_{0.5}MnO_3$ [15]).

(ii) The magnetoresistance at $\mu_0 H = 8$ T is absolutely insignificant over the whole temperature range.

Figure 1(b) displays the magnetic susceptibility χ and its inverse for the 5 K $\leqslant T \leqslant$ 350 K temperature interval. Above $T_N \approx 155$ K, the straight line shown in figure 1(b) is the best fit to the Curie law ($\chi = C/(T - \theta_C)$), which yields $\theta_C = -85$ K and $\mu_{eff} = 7\ \mu_B$. It is thus evidenced that in the paramagnetic regime the fluctuating magnetic moments present dominant AFM correlations. Since AFM interactions between the Mn ions can only occur concomitantly with the existence of OO, this can be interpreted as an indication that such order is present in the system at least below 350 K. The paramagnetic regime ends (when cooling) at $T_N \simeq 155$ K, below which an AFM ordering of the magnetic moments takes place. Again, from susceptibility data, no transitions are evidenced on cooling between T_N and 350 K. Hence, resistivity and susceptibility data for $Bi_{0.5}Sr_{0.5}MnO_3$ confirm a singular behaviour compared to that of the previously studied $Ln_{1/2}Sr_{1/2}MnO_3$—namely, the absence of both (a) a transition to a FM metallic ground state (as in $La_{1/2}Sr_{1/2}MnO_3$) and (b) a transition to a CO/OO state with $T_{CO} < 350$ K (as in many $Ln_{1/2}Sr_{1/2}MnO_3$ compounds with $R_{Ln} < R_{La}$).

In the following we will focus on diffraction results. SXRPD and NPD data taken at RT have been jointly refined by the Rietveld method. These refinements have evidenced that at RT (and below) two phases coexist in the sample studied. The high-resolution diffraction patterns can be satisfactorily reproduced ($R_{wp} < 7\%$ in all cases) using orthorhombic cells, with the *Pbnm* space group for both phases. One of the phases is the majority (60% wt versus 40% wt). Figure 2 shows the NPD refined pattern at RT. The inset (in figure 2) illustrates the presence of the secondary phase. The reflections indexed in the inset correspond to the minority phase. Just including the latter, the peaks and the observed intensities are correctly reproduced. The presence of diffracted intensity of magnetic origin at low temperature agrees with the Néel transition detected in the susceptibility. Interestingly, analysis of the NPD patterns collected

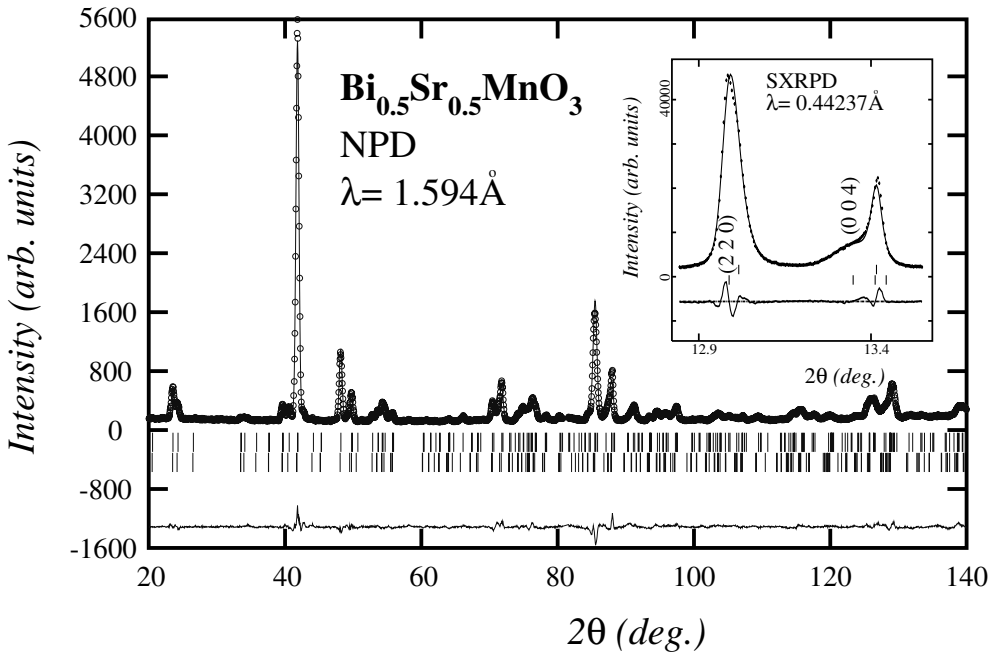

Figure 2. Rietveld refinement of D2B data collected at RT using two phases with the *Pbnm* space group. The inset shows a selected portion of the refined SXRPD pattern (joint refinement) at the same temperature. The indexed peaks correspond to the minority phase.

at $T = 1.5$ K confirms that the two phases present different magnetic structures. For the majority phase the magnetic structure corresponds to the well known CE-type order of Mn moments. This magnetic ordering is characteristic and has only been observed in CO ($x \approx 1/2$) manganites [1]. The observed magnetic order for the minority phase is the A-type magnetic structure. There is a large body of evidence that macroscopic phase segregation is commonly observed in $Ln_{1/2}Sr_{1/2}MnO_3$ manganites [17] (even in samples with compositional fluctuations lower than 2%) due to the energies of CE-type and A-type phases being very similar.

The above arguments can be taken as indirect proofs of the existence of CO and OO in the majority phase of the $Bi_{0.5}Sr_{0.5}MnO_3$ sample over the whole range of temperatures studied (up to 350 K). Furthermore, the existence of the CO/OO state is confirmed unambiguously by the presence of superlattice reflections, already identifiable at RT from SXRPD data. Figure 3 shows the two most intense superlattice peaks. They correspond to a modulation wave vector $\boldsymbol{k} = (0, 1/2, 0)$ in the $Pbnm$ setting. It is of interest that these peaks can only be indexed with lattice parameters $a \times 2b \times c$ of the majority phase, which displays CE-type ordering and a $2a \times 2b \times c$ magnetic cell.

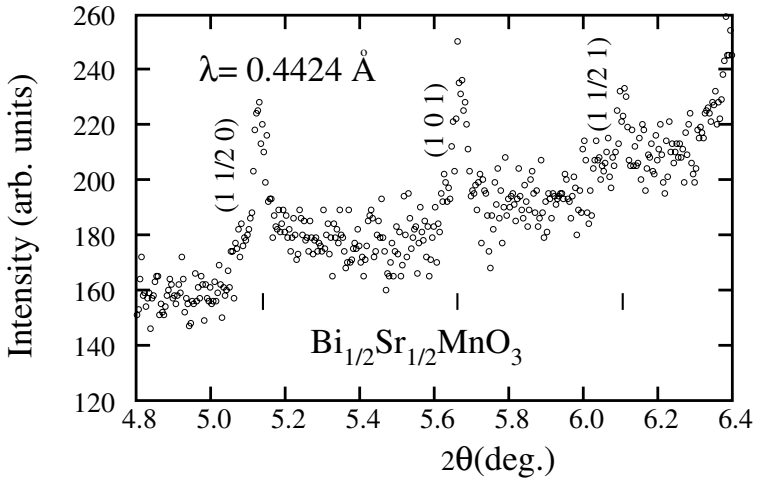

Figure 3. (1 1/2 0) and (1 1/2 1) superlattice peaks at RT, from SXRPD data.

Since very few superlattice reflections are observed, it is not possible to refine the whole supercell structure. Only the average $Pbnm$ cell was refined. The lattice parameters, Mn–O bond distances, and Mn–O–Mn bond angles obtained using the average $Pbnm$ description for each phase are listed in table 1. Both phases present a considerable compression of the c-axis. This compression can be quantified through the parameter ϵ_c defined as

$$\epsilon_c \equiv \frac{\sqrt{2}c}{a+b}.$$

The compression, which is usual in the CO and/or OO manganites, arises from the localization of the e_g electrons in the ab-planes ($Pbnm$ setting). The analysis of the ϵ_c-deformation reveals two significant features:

(i) ϵ_c for the majority phase ($\epsilon_c = 35$) is larger than for other half-doped manganites showing CO (for instance, $\epsilon_c = 26$ for $La_{0.5}Ca_{0.5}MnO_3$ at 1.5 K [19] and $\epsilon_c = 23$ for $Nd_{0.5}Ca_{0.5}MnO_{3.02(1)}$ at 1.5 K [18]); and
(ii) this parameter is almost constant over the temperature interval 1.5 K $\leqslant T \leqslant$ 300 K.

Table 1. Structural parameters obtained by Rietveld refinement of NPD and SXRPD data at RT and $T = 1.5$ K. Phase 1 is the majority phase and phase 2 is the minority one. O1 stands for the oxygen in the apical positions and O2 for the oxygen in the basal positions. The R_{wp}-factors are always below 7%.

	$T = 300$ K		$T = 1.5$ K	
	Phase 1	Phase 2	Phase 1	Phase 2
a (Å)	5.5263(2)	5.5358(1)	5.5313(5)	5.5299(6)
b (Å)	5.5139(2)	5.5261(2)	5.5063(4)	5.5207(8)
c (Å)	7.5733(1)	7.6133(3)	7.5307(4)	7.5918(8)
$\epsilon_c \equiv \left\lvert 1 - \frac{\sqrt{2}c}{a+b} \right\rvert \times 10^3$	30	27	35	29
$d_{\mathrm{Mn-O1}}$	1.913(1)	1.934(1)	1.900(1)	1.930(2)
$\langle d_{\mathrm{Mn-O2}} \rangle$	1.961(1)	1.968(3)	1.964(3)	1.966(2)
$\langle d_{\mathrm{Mn-O}} \rangle$	1.945(1)	1.957(2)	1.964(3)	1.966(2)
$\epsilon_d \equiv \left\lvert 1 - \frac{d_{\mathrm{Mn-O1}}}{\langle d_{\mathrm{Mn-O2}} \rangle} \right\rvert \times 10^4$	245	170	326	181
$\theta_{\mathrm{Mn-O1-Mn}}$	163.6(3)	159.4(4)	164.6(1)	159.0(1)
$\theta_{\mathrm{Mn-O2-Mn}}$	168.7(2)	166.9(3)	167.0(5)	167.1(7)
$\langle \theta_{\mathrm{Mn-O-Mn}} \rangle$	166.9(2)	164.4(3)	166.2(6)	164.4(7)

The same behaviour is observed for the apical compression of the MnO_6 octahedra. This compression can be quantified through the parameter ϵ_d defined as

$$\epsilon_d \equiv \left| 1 - \frac{d_{\mathrm{Mn-O1}}}{\langle d_{\mathrm{Mn-O2}} \rangle} \right| \times 10^4.$$

We observe that the average deformation of the octahedra is also larger than for the aforementioned CO samples ($\epsilon_d = 245$ (majority phase) and 170 (minority phase) for $Bi_{0.5}Sr_{0.5}MnO_3$ at RT; $\epsilon_d = 205$ for $La_{0.5}Ca_{0.5}MnO_3$ [19] and $\epsilon_d = 217$ for $Nd_{0.5}Ca_{0.5}MnO_{3.02(1)}$ at 1.5 K [18]). Although its relative variation from 300 K to 1.5 K is appreciable, it is much smaller than for other compounds presenting CO [18, 19].

Finally, the stability of the CO state was found to be notably high. We have investigated the stability of the two coexisting low-temperature states in the $Bi_{0.5}Sr_{0.5}MnO_3$ sample by means of magnetization measurements up to 50 T. The high stability of the CO/OO phase is evidenced by the $M(H)$ curve taken at $T = 4$ K which is presented in figure 4. It is noteworthy that a field of 50 T is not enough to completely saturate the magnetization ($M_{\mathrm{sat}} = 3.5\ \mu_B$), and therefore it is not sufficient to melt the CO state. This behaviour is in great contrast with, for instance, that of $La_{1/2}Ca_{1/2}MnO_3$. The average distortion of $La_{1/2}Ca_{1/2}MnO_3$ is clearly more pronounced ($\langle\theta\rangle = 161.2^\circ$) than in $Bi_{0.5}Sr_{0.5}MnO_3$. Nevertheless, the melting of the CO/OO state in the former occurs at a critical field $\mu_0 H_c \approx 8$ T, well below the field necessary to induce the transition in the latter ($\mu_0 H_c > 45$ T, according to figure 4).

4. Conclusions and summary

The structural information gathered in table 1 demonstrates that, throughout the temperature range (below RT), the two coexisting phases present a confinement of the e_g electrons in the ab-planes, the signature of OO in half-doped manganites. This order is responsible for the AFM correlations of the magnetic moments evidenced by the $\chi(T)$ curve. That OO and CO already exist at RT is directly confirmed by the superlattice peaks associated with $\boldsymbol{k} = (0, 1/2, 0)$ structural modulation. At low temperature, the CE-type magnetic order found for the majority

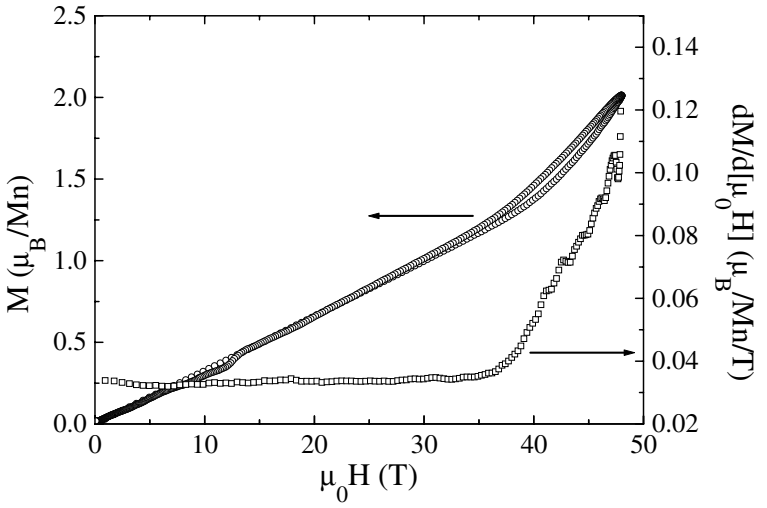

Figure 4. Magnetization as a function of the applied magnetic field up to 50 T at $T = 4$ K.

phase also reinforces the assertion that it presents both OO and CO. The great similarity of the structural parameters (table 1) found at 1.5 K and at 300 K, together with the absence of transitions in the electrical resistivity and magnetic susceptibility from T_N to 350 K, provides evidence that CO is also present at 350 K. This is unambiguously confirmed by the presence of superlattice reflections at RT.

In summary, the $Bi_{0.5}Sr_{0.5}MnO_3$ oxide investigated presents two-phase coexistence at RT. Both phases present OO throughout the whole interval 1.5 K $\leqslant T \leqslant$ 350 K, and the majority phase presents CO. These results are quite unexpected, mainly for two reasons:

(i) the largest value of T_{CO} ever reported for a Sr-half-doped manganite is 165 K (for $Nd_{0.4}Sm_{0.1}Sr_{0.5}MnO_3$ [10]); and
(ii) T_{CO} for the more distorted $Bi_{0.5}Ca_{0.5}MnO_3$ is 325 K [20], lower than for the Sr-doped bismuth-based manganite.

Acknowledgments

This work was done with financial support from the CICyT (MAT97-0669), MEC (PB97-1175) and Generalitat de Catalunya (GRQ95-8029). AL acknowledges financial support from the Oxide Spin Electronics Network (EU TMR) programme. The ILL and ESRF are acknowledged for making beam time available.

References

[1] Wollan E O and Koehler W C 1955 *Phys. Rev.* **100** 545
[2] Goodenough J B 1955 *Phys. Rev.* **100** 564
[3] Kanamori J 1959 *J. Phys. Chem. Solids* **10** 87
[4] Rao C N R, Arulraj A, Santosh P N and Cheetham A K 1998 *Chem. Mater.* **10** 2714
[5] Fontcuberta J, Martínez B, Seffar A, Piñol S, García-Muñoz J L and Obradors X 1996 *Phys. Rev. Lett.* **76** 1122
[6] Shannon R D 1976 *Acta Crystallogr.* A **32** 751
[7] Ritter C, Ibarra M R, De Teresa J M, Algarabel P A, Marquina C, Blasco J, García J, Oseroff S and Cheong S-W 1997 *Phys. Rev.* B **56** 8902

[8] Atou T, Chiba H, Ohoyama K, Yamaguchi Y and Syono Y 1999 *J. Solid State Chem.* **145** 639
[9] Righi L, Amboage M, Guitiérrez J, Barandiarán J M, Fernández-Barquín L and Fernández-Díaz M T 2000 *Physica* B **276–278** 718
[10] Kuwahara H, Moritomo Y, Tomioka Y, Asamitsu A, Kasai M, Kumai R and Tokura Y 1997 *Phys. Rev.* B **56** 9386
[11] Larson A C and Von Dreele R B 1994 *Los Alamos National Laboratory Report* No LA-UR-86-748
[12] Rodríguez-Carvajal J 1993 *Physica* B **192** 55
[13] Kawano H, Kajimoto R, Yoshizawa H, Tomioka Y, Kuwahara H and Tokura Y 1997 *Phys. Rev. Lett.* **78** 4253
[14] Caignaert V, Millange F, Hervieu M, Suard E and Raveau B 1996 *Solid State Commun.* **99** 173
[15] Vanitha P V, Singh R S, Natarajan S and Rao C N R 1998 *J. Solid State Chem.* **137** 365
[16] Schiffer P, Ramirez A P, Bao W and Cheong S-W 1995 *Phys. Rev. Lett.* **75** 3336
[17] Woodward P M, Cox D E, Vogt T, Rao C N R and Cheetham A K 1999 *Chem. Mater.* **11** 3528
[18] Frontera C, García-Muñoz J L, Llobet A, Ritter C, Alonso J A and Rodríguez-Carvajal J 2000 *Phys. Rev.* B **62** 3002
[19] Radaelli P G, Cox D E, Marezio M and Cheong S-W 1997 *Phys. Rev.* B **55** 3015
[20] Cheong S-W and Chen C H 1998 *Colossal Magnetoresistance, Charge Ordering and Related Properties of Manganese Oxides* ed C N R Rao and B Raveau (Singapore: World Scientific)